# INFERRING THE ROUGHNESS OF DESERT ROCKY SURFACES FROM THEIR BIDIRECTIONAL REFLECTANCE DATA

A. Karnieli [1] and J. Cierniewski [2]

[1]*Jacob Blaustein Institute for Desert Research, Ben Gurion University of the Negev, 84990, Israel*
[2]*Institute of Physical Geography and Environmental Planning, Adam Mickiewicz University, Fredry 10, 61-701 Poznań, Poland*

## ABSTRACT

Bare soil surfaces show variation in their upward radiance depending on the direction of irradiating solar energy and the direction along which the reflected energy is viewed. Desert surfaces can exhibit both a backscattering and forward scattering characteristics. The authors tried to infer the roughness of desert rocky surfaces from their bidirectional reflectance data sets, using a geometrical reflectance model inversion technique. To achieve this, virtual equivalents of the surfaces were generated. These virtual surfaces simulate real surfaces with equal-sized opaque spheroids regularly dispersed on freely sloping plane. The capabilities of the model inversion were tested on semiarid surfaces of the Negev desert including rough rocks and smooth dune sands.
© 2001 COSPAR. Published by Elsevier Science Ltd. All rights reserved.

## INTRODUCTION

Desert gypsum and quartz sands display a high reflectance and maximum forward scattering in the optical domain (Coulson, 1966). The forward scattering, as well as the backward scattering characteristics of a dune sand surface and an alkali flat bare soil have been observed by Deering *et al.* (1990). Shoshany (1993) found that most of the desert stone pavements and rocky surfaces produce anisotropic reflection with a clear backscattering regime. Most geometrical soil directional reflectance models have treated directly illuminated soil surface fragments as perfect diffuse reflectors. The model of Norman *et al.* (1985) simulates soil aggregates with cuboids. In the Monte Carlo reflectance model of Cooper and Smith (1985) the soil surface is described with a cosine function in one or two directions. The models of Cierniewski (1987) and Irons *et al.* (1992) describe soil aggregates with regularly spaced equal-sized spheres. The latest improved version of Cierniewski's models (1999) simulates soil aggregates with spheroids. It also takes into account the specular features of the soil surfaces.

The aim of the paper is to apply the inversion of this latest model to infer the roughness of desert rocky surfaces from their bidirectional reflectance data sets. Virtual surfaces are used as input data for the model. They describe the geometry of the surfaces and their reflectance features, and are discussed on the background of their real equivalents.

## METHODS
### The model

The model considers a soil surface as equal-sized opaque spheroids, of horizontal and vertical semi-axes $a$ and $b$ dispersed in a net of squares of side $d$ (Fig.1). They are absorbed into the plane, their tops projecting to a height $t$ above it. The structure is illuminated by direct solar beams at zenith and azimuth angles $\theta_s$ and $\phi_s$, as well as diffuse light, $f_{di}$, defined as the part of the energy from the direct solar beams. A sensor is suspended over the simulated soil surface. It observes the surface along the solar principal plane *(SPP)* at zenith angles $\theta_v$ in the forward scattering and backscattering directions. The sensor, with field-of-view defined by the angle $\alpha$, is located at a distance $h$ away from the observed surface. The amount of wave energy coming directly to the illuminated individual facet of the geometrical structure defines the factor $Ei_v{}^{\downarrow}{}_{fa}$:

$$Ei_v{}^{\downarrow}{}_{fa} = \cos\theta_s\cos\beta + \sin\beta + \sin\theta_s\cos(\phi_r - \phi_s),\qquad(1)$$

where: $\beta$ is the slope angle of the facet, and $\phi_r$ and $\phi_s$ are the azimuth angles describing the position of the facet and the Sun, respectively. The value of this factor $Ei_v^{\downarrow}{}_{fa}$, equals the cosine of the incidence angle $\gamma_i$ of the direct solar beams to the facet, measured with respect to its normal. It expresses the vector length of the energy leaving the facet along the normal. The energy leaving the directly illuminated facets $Ei_v^{\uparrow}{}_{fa}$ is directly proportional to the energy incident on it $Ei_v^{\downarrow}{}_{fa}$. The $Ei_v^{\uparrow}{}_{fa}$ is in part perfectly diffused, and in part reflected in a specular way. The model assumes that the length of the reflected energy vector in a given direction $\theta_v$ is the sum of the length of these two vectors: the perfectly diffused energy $Edi_{(\theta_v)}^{\uparrow}{}_{fa}$ and the energy specularly reflected $Esp_{\theta_v}^{\uparrow}{}_{fa}$ (Fig. 2):

The length of the vector $Esp_{\theta_v}^{\uparrow}{}_{fa}$, describing unpolarised light, depends on polarisation $Fp_{(\gamma)}$ of the reflected light $Ei_v^{\downarrow}{}_{fa}$ at the $\gamma_i$ angle, as:

$$Esp_{\theta_v}^{\uparrow}{}_{fa} = Ei_v^{\uparrow}{}_{fa} \cdot Fp_{(\gamma_i)}; \quad Fp_{(\gamma_i)} = \frac{r_{\perp}^2 + r_{=}^2}{2}, \qquad (2)$$

where: $r_{\perp}$ and $r_{=}$ are respectively the perpendicular and parallel Fresnel reflection coefficient, given by:

$$r_{\perp} = \frac{-n^2 \cos\gamma_i + \sqrt{n^2 - \sin^2\gamma_i}}{n^2 \cos\gamma_i + \sqrt{n^2 - \sin^2\gamma_i}} \quad ; \quad r_{=} = \frac{\cos\gamma_i - \sqrt{n^2 - \sin^2\gamma_i}}{\cos\gamma_i + \sqrt{n^2 - \sin^2\gamma_i}},$$

where $n$ is the refractive index the soil surface. The vector of the energy specularly reflected is oriented in that way that the angle of incidence, $\gamma_i$, equals the angle of reflection, $\gamma_r$. As the vector of the quasi-specular reflected energy, it is visible inside the limited angle range defined by the $2\partial$ angle around the direction of reflection.

The diffuse light $Esk^{\downarrow}{}_{fa}$ reaches the soil surface fragments directly illuminated by the sun beams, as well as the shaded fragments. Its amount is limited by presence of adjoining the spheroids, which reduce the amount of diffuse energy relative to the condition when it comes from the complete hemisphere (Fig. 3):

$$Esk^{\uparrow}{}_{fa} = f_{di} \frac{\delta}{180°}, \qquad (3)$$

where $f_{di}$ approximates a reflectance effect from soil surfaces illuminated only by the diffuse light component.

The radiance factor of the simulated soil surface with directly illuminated and shaded fragments, viewed by the sensor from a given direction $\theta_v$ along a given profile $pr$, is defined as:

$$L_{\theta_v}^{\uparrow}{}_{pr} = \sum_{i=1}^{j} \left[ \left( Eis_{\theta_v}^{\uparrow}{}_{fa_{(i)}} + Esk^{\uparrow}{}_{fa_{(i)}} \right) \xi\, i_{fa_{(i)}} \right] + \sum_{i=1}^{j} \left( Esk^{\uparrow}{}_{fa_{(i)}} \cdot \xi\, s_{fa_{(i)}} \right), \qquad (4)$$

where $i$ is $i$th facet of the geometrical structure, $\xi\, i_{fa(i)}$ and $\xi\, s_{fa(i)}$ are the elementary view angles of the illuminated and the shaded $i$th facet, respectively. The radiance of the simulated soil surface reaching the sensor through its field-of-view $L_{\theta_v}^{\uparrow}{}_{FOV}$ is the mean values calculated along the individual profiles $L_{\theta_v}^{\uparrow}{}_{pr}$ and the space between the spheroids.

Finally, the reflectance from a rough soil surface along the solar principal plane $SPP$ is described by the normalised reflectance $NR_{(\phi_v, SPP, \theta_v)}$, which is defined as the ratio of the total radiance $L_{\theta_v}^{\uparrow}{}_{FOV}$ measured from the off-nadir direction $\theta_v$ to the radiance measured from the nadir.

Assuming that the soil normalised reflectance $NR_{(\phi_v, SPP, \theta_v)}$ in the plane $OP$ perpendicularly oriented to the $SPP$ for each of the view zenith angle $\theta_v$ is 1 and the distribution of the ratio in the function of the $\phi_v$ between the $SPP$ and the $OP$ is a simple line one, its value $NR_{(\phi_v, \theta_v)}$ for any observation plane can be defined as:

$$NR_{(\phi_v, \theta_v)} = NR_{(\phi_v = SPP, \theta_v)} \left( 1 - \frac{\phi_v}{90°} \right) + \frac{\phi_v}{90°}, \qquad (5)$$

where $\phi_v$ is the relative horizontal angle of the observation plane measured from the $SPP$.

## Fitting of the virtual surface geometry

The model inversion was applied to infer the geometry of five rocky surfaces and dune sand using sets of their directional reflectance measurements. The directional reflectances from the surfaces were measured with a field radiometer CIMEL 313-21. The instrument, which has a 10° field of view, recorded the radiance in 4 wavelength
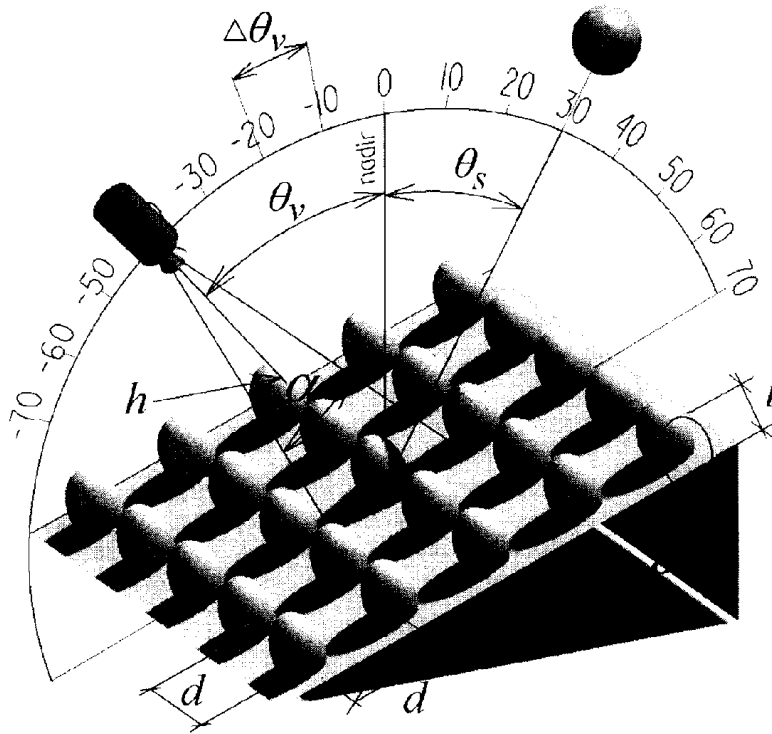
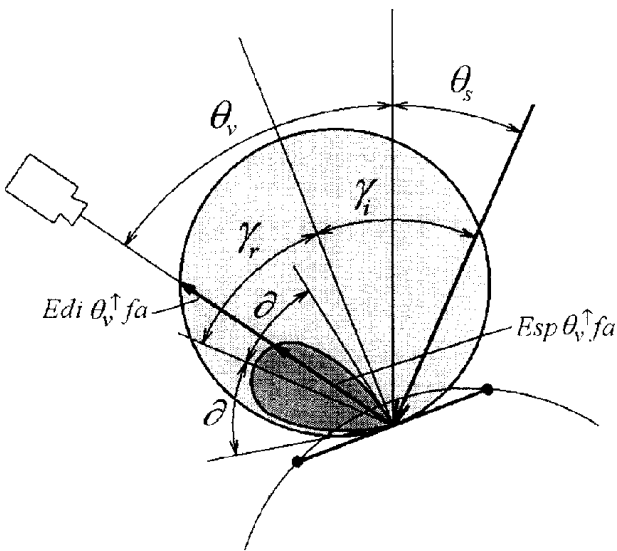Fig. 1. Schema of the model representation.



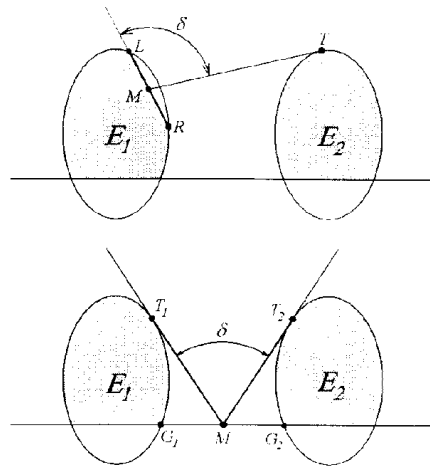Fig. 2. Distribution of the energy leaving a facet in the specular and the diffuse way.



Fig. 3. Limitations in illumination by skylight of the facet segment $LR$ on the ellipse $E_1$ and the slope plane between ellipses $E_1$ and $E_2$, expressed by the angle $\delta$. $M$ is the middle point of the segments $LR$ and $G_1G_2$. $T$, $T_1$ and $T_2$ are the tangent points from the sides to the neighbouring ellipses forming the angle $\delta$.

bands ranging between 550 nm and 1650 nm. It collected the data along the *SPP* from a distance of 2.5 m between 70° towards the Sun, through the nadir, to 70° away from the Sun, at 10° increments. The data were acquired under clear sky conditions at least seven solar zenith angles $\theta_s$ for each surface, varied from 8° to 72°.

Based on the geometrical parameters of the studied surfaces, virtual surfaces were reconstructed using the model. This was done by choosing those values of the $b$, $d$, $t$ geometrical parameters (completed by the $n$ and $f_{di}$ for a given wavelength), which gave the lowest possible root mean square error (*rms*) between the distribution of the soil *NR* measured as a function of view zenith angle and that predicted by the model. The average horizontal semi-axis $a$ of the spheroids was evaluated from photographs. Other parameters describing the conditions of illumination and observation of the studied soil surfaces, $\theta_s$, $h$, $\alpha$, were taken from measured values.

This fitting was performed automatically using a special computer procedure. A program, written in Object Pascal, automatically fits the geometrical parameters of the analysed soil surfaces. It is realised in two stages. In the first one, for a surface at each solar zenith angle $\theta_s$, the program computes the $rms_{\theta_s.s}$ using the following formula:

$$rms_{\theta_s.s} = \frac{1}{nv-1}\sqrt{\sum_{nv-1}^{nv}\left(M_{\theta_s,\theta_v} - P_{\theta_s,\theta_v,s}\right)^2}, \tag{6}$$

where $nv$ is the number of $\theta_v$, $M_{\theta_s, \theta_v}$ is a measured value of the *NR* for given angles $\theta_s$ and $\theta_v$, $P_{\theta_s, \theta_v, s}$ is a predicted value of *NR* for these both angles and the set $s$ of parameters: $b$, $t$, $d$, $n$ and $f_{di}$. Those pairs, for which the measured data were collected in the situation when the luminancemeter cast a shadow on the observed surface, were eliminated from the calculation. In the second stage the program determines the qualities $K_s$:

$$K_s = \sum rms_{\theta_s,s}, \tag{7}$$

where the sum is spread over all values of $\theta_s$. Finally, the minimum value among $K_s$'s is found and it indicates the set $s$ for which the average root mean square is the lowest.

## RESULTS AND THEIR DISCUSSION

This research was conducted in the northern Negev desert (Israel). The study sites are characterized by various mixture of soils and rocks. These include reg soils, which are also denoted as desert pavement. Gravel and flint fragments from the Senonian age are the product of *in situ* weathering cover of the bedrock. The rocks size, which is of the order of a few centimeters in diameter, varies from site to site. Loess soils occur in the interstices between the rocks of the pavement. Thus, the rocks are partially submerged beneath the surface and partially exposed. Two of the rough rocky surfaces and their virtual equivalents are presented in Figure 4, together with the sand surfaces. The virtual surface of the dune sands is essentially different in terms of the size of its irregularities and its shape compared to the virtual rocky surfaces (table 1). The spheroids representing the virtual sands are almost spherical, like natural quartz grains. They are the least absorbed into the ground and nearly touch each other. The spheroids of the virtual rocky surfaces are much more vertically elongated and absorbed deeper into the ground. The *NR* curves generated by them display a reflectance peak in the backscattering directions and minimum reflectance in the forward scattering range. The virtual structures simulating the reflectance from surfaces covered by larger rocks have larger flat spaces between emerged tops of the spheroids. As a result of the larger proportion of those

Table 1. Parameters of the virtual surfaces and the average root mean square error (*rms*) for 850 nm corresponding to them

| Surface | $a$ (cm) | $b/a$ | $t/a$ | $d/a$ | $n$ | *rms* |
|---------|----------|-------|-------|-------|-----|-------|
| Sandy | 0.025 | 1.1 | 0.7 | 2.00 | 1.9 | 0.013 |
| Rocky (A) | 1.0 | 4.0 | 0.8 | 1.75 | 2.3 | 0.023 |
| Rocky (B) | 1.2 | 5.0 | 0.9 | 1.70 | 2.3 | 0.027 |
| Rocky (C) | 2.1 | 8.0 | 0.9 | 1.70 | 2.3 | 0.024 |
| Rocky (D) | 3.5 | 8.0 | 0.9 | 2.10 | 2.3 | 0.026 |
| Rocky (E) | 7.5 | 8.0 | 0.7 | 1.90 | 2.3 | 0.026 |

$f_{di} = 0.05$.

## Sandy surface



### Rocky surface (B)
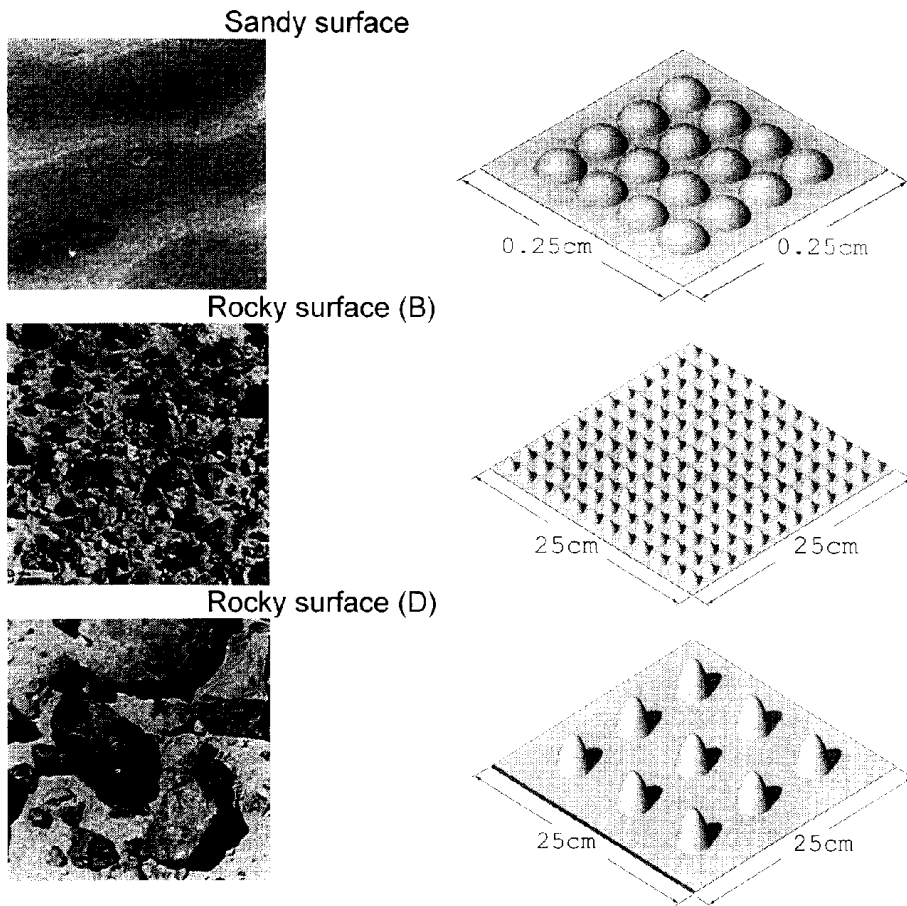


### Rocky surface (D)



Fig. 4. Close-up view of the studied surfaces 25X25 cm (left) and their virtual equivalents (right).

flat fragments of the virtual surfaces, the $NR$ curves generated by them are more flattened than the curves for surfaces with smaller rocky material (Fig. 5). Also, the more flattened tops of the spherical spheroids of the sand virtual surface enable us to generate the lowest variation of its $NR$ as a function of view zenith angle $\theta_v$. Comparing the $NR$ curves of the sand surface with those representing the rocky surfaces, the former curves are flatter with a minimum equal to 1 near the view zenith angle $\theta_v = 0°$. This means that the dune sand surfaces are appear darker when viewed at nadir.

The accuracy of the fitting $b$, $t$, $d$, $n$ and $f_{di}$ parameters of the five rocky virtual surfaces was evaluated by analysing the reflectance data for 41 pairs of the $NR$ curves related to them, generated by the model and measured with the radiometer. For all of these surfaces the goodness-of-fit, expressed by the coefficient of determination $r^2$, is between 85 per cent and 96 per cent for all spectral bands.

## CONCLUDING REMARKS

The results show that through the inversion of the geometrical model discussed in the paper, it is possible to infer the roughness of rocky surfaces with satisfactory precision. The reconstruction of the geometry of those surfaces using sets of their directional reflectance measurements in the optical domain, collected along the solar principal plane at several solar zenith angles, enable us to distinguish some states of their roughness. The studied surfaces are described by sets of four geometrical parameters: the horizontal and vertical semi-axes of spheroids, the height of their tops above the slope plane and the distance between the spheroids These parameters sets, completed by the refractive index of the simulated surfaces (also referred to as virtual surfaces), give possibilities to predict the directional reflectance of the surfaces under any illumination and viewing conditions. The authors expect that a similar procedure can be also useful for the reconstruction of the geometry of extraterrestrial surfaces.
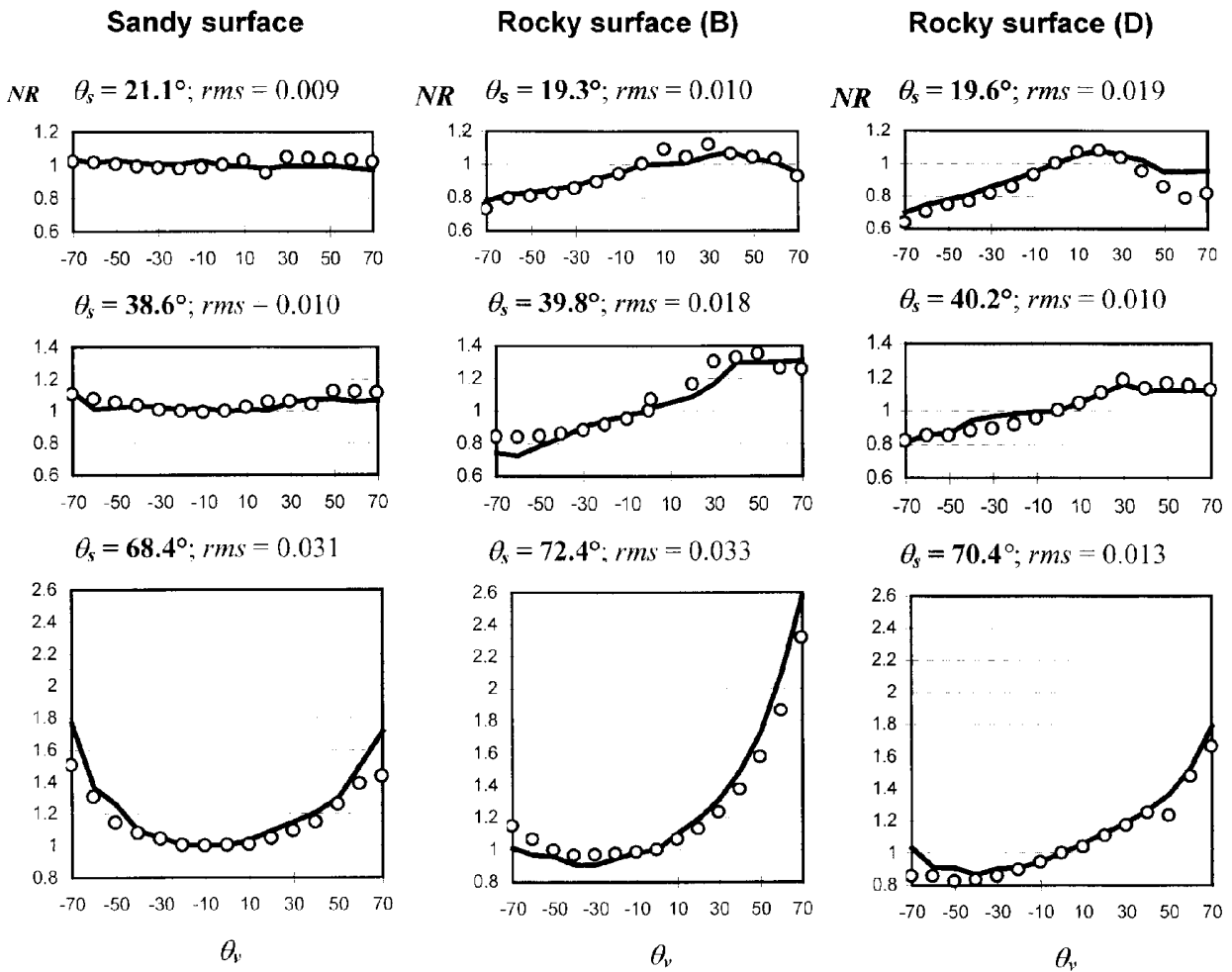
A. Karnieli and J. Cierniewski



Fig. 5. Relation between the normalised reflectance *NR* of the studied surfaces along the solar principal plane at 850 nm predicted by the model (line) and measured (points) for selected solar zenith angles $\theta_s$. Negative view zenith angle $\theta_v$ values correspond to forwardscattering directions, while positive angular values designate backscattering directions. *rms* is the root mean square error for measured and the model generated *NR* data.

## REFERENCES

Cierniewski, J., A model for soil surface roughness influence on the spectral response of bare soils in the visible and near-infrared range, *Remote Sensing of Environment*, 23, 97-115, 1987.

Cierniewski, J., Geometrical modelling of soil bidirectional reflectance in the optical domain, Bogucki Scientific Publishers, Poznań, 1999.

Cooper K.D. and J.A.Smith, A Monte Carlo reflectance model for soil surfaces with three-dimensional structure. *IEEE Transactions on Geosciences and Remote Sensing*, 1GE-23, 668-673, 1985.

Coulson, K. L., Effects of reflection properties of natural surfaces in aerial reconnaissance. *Applied Optics*, 5, 905-917, 1966.

Deering, D. W., T. F. Eck., and J. Otterman, Bidirectional reflectance of selected desert surfaces and their three-parameter soil characterization, *Agricultural and Forest Meteorology*, 52, 71-90, 1990.

Irons, J. R., G. S. Campbell, J. M. Norman, D. W. Graham, and W. M. Kovalick, Prediction and measurement of soil bidirectional reflectance, *IEEE Transations on Geoscience and Sensing*, 30, 249-260, 1992.

Norman J. M., J. M. Welles and E. A. Walter, Contrast among bidirectional reflectance of leaves, canopies, and soils. *IEEE Transactions on Geosciences and Remote Sensig*, 1GE-23, 659-667, 1985.

Shoshany, M., Roughness-reflectance relationship of bare desert terrain: An empirical study, *Remote Sensing of Environment*, 45, 15-27, 1993.